

DESIGN OF WIRELESS ULTRA-WIDEBAND COMMUNICATION SYSTEMS

by
**Domenic Forte
&
Julia Tu**



**University of Maryland at College Park
Electrical and Computer Engineering Department
Maryland Engineering Research Internship Teams 2005**

Acknowledgements

This project was supported by the ECE Department of the University of Maryland MERIT 2005 program, the National Science Foundation, and the Army Research Laboratory.

Special thanks to Dr. K.J.Ray Liu, Dr. Jaemin Ahn, Hung-Quoc Lai, Wipawee Siriwongpairat and Thanoongsak Himsoon for their assistance.

Table of Contents

List of Illustrations	ii
Abstract	1
Introduction	2
Methods and Materials	4
▪ Orthogonal Frequency Division Multiplexing	4
▪ Multipath and Inter-Symbol Interference	5
▪ UWB System	6
▪ SISO, MISO, and MIMO UWB Systems	9
▪ UWB Standard Channel Models and Channel Estimation	10
▪ Matlab Implementation	11
Results	13
Discussion	18
Conclusion	20
Appendix	22
References	24

List of Illustrations

Table:

Table 1.....	6
--------------	---

Figures:

Figure 1.....	2
Figure 2.....	5
Figure 3A.....	6
Figure 3B.....	7
Figure 4A,B.....	8
Figure 5.....	9
Figure 6 A,B,C,D.....	14
Figure 7 A,B,C,D.....	15
Figure 8 A,B.....	15
Figure 8 C,D.....	16
Figure 9 A,B.....	16
Figure 9 C,D.....	17
Figure 10 A,B,C,D.....	17
Figure 11 A,B,C,D.....	18

Abstract

This project explores the innovative Ultra-Wideband (UWB) technology for indoor wireless communications with ten different data rates ranging from 53.3 Mbps to 480 Mbps. The software that includes all of the algorithms deployed at both transmitter and receiver sides is extended further to take Inter-Symbol Interference distortions as well as channel estimation into account for more realistic simulations. The bit error rate performance of three different types of UWB systems: single-input single-output (SISO), multiple-input single-output (MISO), and multiple-input multiple-output (MIMO) under four standard channel models is investigated. Simulation results show that the UWB-MIMO system outperforms the other systems since it inherits the highest spatial diversity gain of four due to its antenna schemes.

Introduction

According to the Federal Communication Commission (FCC) [3], any transmission that occupies a bandwidth of more than 500 MHz is called Ultra-Wideband (UWB). The FCC has also mandated that UWB transmission can legally operate in the range from 3.1 GHz to 10.6 GHz, at a transmit power of -41dBm/MHz as shown in Figure 1. The power is limited because the UWB must coexist with modern wireless schemes such as narrowband 802.11a [5]. The power constraint also means that UWB devices can only operate in a short range of 10 meters (about 33 feet) [6].

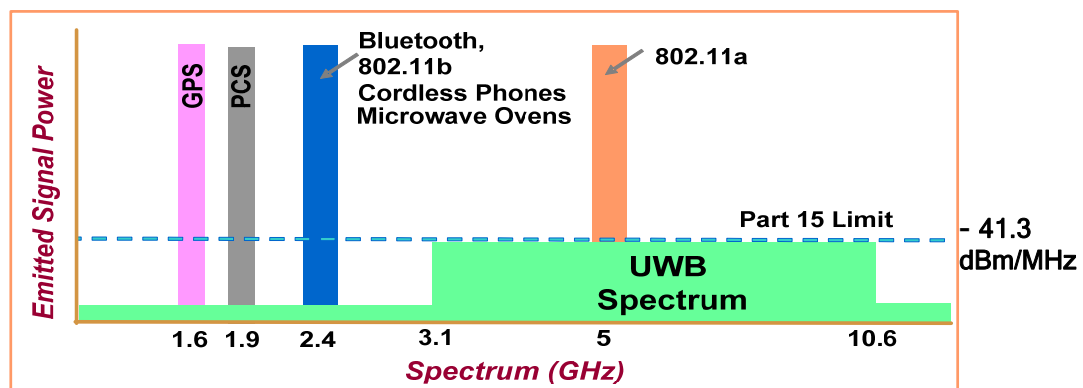


Figure 1: Frequency spectrum of UWB and existing narrowband systems [7].

Modern UWB systems use modulation techniques, such as Orthogonal Frequency Division Multiplexing (OFDM) [2], to occupy a wide bandwidth. The use of multiple bands in combination with OFDM modulation can provide significant advantages to traditional UWB systems. OFDM is best suited for frequency selective channels and high data rate transmission [4]. The difference between the multiband and the conventional OFDM is that the symbols are not continuously transmitted on only one band. Instead, they can be interleaved across subbands. OFDM modulates data in each subband per transmission transforming the frequency-selective wide-band channel into a group of non-selective narrowband channels. OFDM also reduces the complexity and cost of a single carrier system with its clever use of cyclic redundancy [4].

UWB brings the convenience and mobility of wireless communications to high-speed connections for various devices and applications including the Universal Serial Bus (USB) port. Recently, an upgraded high-speed USB was released to support a high data

rate of 480 Mbps for multimedia and storage applications. Since most of current USB devices are wired, consumers are limited by the maximum cable length of 5 meters (approximately 16 feet) in the current USB standard. Additionally, it can often be a hassle to connect every USB device at the office or at home to a computer. Existing wireless schemes including Bluetooth and IEEE 802.11/a/b/g are limited in terms of transmission rates making UWB the most viable candidate for short range communications in dense multipath environments. Due to its bandwidth, a UWB system has the potential for high-capacity to accommodate many users in multipath environments with minimal interference.

By employing UWB, users could set up and connect all the components for an entire home entertainment center with greater ease. For example, one would be able to stream video content from a PC or consumer electronics device like a video recorder to a television display without the need for a cable. The UWB system can also be implemented inexpensively since transceivers do not require mixers or a power amplifier.

However, there are still many challenges associated with UWB technology making it more difficult to test and implement. The limits on transmit power spectral density due to FCC requirements will most likely cause the UWB system to experience narrowband interference making interference suppression techniques a necessity. In addition, sacrifices in time and frequency diversity must be made in order to accommodate higher data rates. Accurate channel models that describe UWB signal propagation and acknowledge multipath components are needed for computer simulations. Channel estimation and other distortions must also be taken into account in order to yield realistic results. For example, Inter-Symbol Interference (ISI) and Inter-Block Interference (IBI) [4] can alter a signal traveling from the transmitter to the receiver.

The behavior of the bit error rate is investigated by transmitting signals at ten different data rates ranging from 53.3 Mbps to 480 Mbps across 4 unique channels with Matlab software to act as the UWB system. Single-input single-output (SISO), multiple-input single-output (MISO), and multiple-input multiple-output (MIMO) UWB systems will be examined to show how the spatial diversity gains of multiple antennas may be used to overcome sacrifices made for higher data rates. By extending the software from

the single-antenna wireless USB architecture to MIMO wireless USB architecture with Alamouti space-time block code [1] to modulate the signal and Tarokh fast maximum likelihood detection [8] to demodulate the signal, multiple transmit and receive antennas in high-speed wireless USB should further improve UWB system performance.

Methods and Materials

Orthogonal Frequency Division Multiplexing

A main concept behind Orthogonal Frequency Division Multiplexing (OFDM) involves transforming a channel convolution in time to a multiplication in the frequency domain [4]. Let $r(t)$ be the received signal, $x(t)$ be the transmitted signal, $h(t)$ be the impulse response, and $w(t)$ be the noise:

$$r(t) = \int_{-\infty}^{\infty} x(\tau)h(t - \tau) + w(t) \quad (1)$$

Then, by using the Fourier Transform of each component, equation 1 can be simplified:

$$R(f) = X(f)H(f) + W(f) \quad (2)$$

In a communication system, one's job is essentially to retrieve the transmitted signal from equation 1 and 2. However, there are certain factors that hinder the accomplishment of the task. Frequency selectivity occurs when the transmitted signal occupies a bandwidth greater than that of the coherence bandwidth of the channel. This results in different gains for the frequency components of the transmitted signal at the receiver. This is also known as fading.

OFDM's best qualities include its high spectral efficiency and tolerance to Inter-Symbol Interference (ISI). OFDM divides a large bandwidth into smaller subcarriers that are mathematically orthogonal. Information can not only be sent on parallel overlapping subcarriers, but also extracted individually. Figure 2 includes the OFDM spectrum where one can see its efficiency. In our multiband UWB system, the frequency band is divided into 14 subbands; each subband occupies a bandwidth of 528 MHz satisfying the FCC's definition of Ultra-WideBand. Each OFDM symbol, modulated using QPSK, is made up of 128 tones with 100 data tones used to transmit information, 12 pilot tones for carrier and phase tracking, 10 guard tones, and 6 NULL tones. By using frequency spread and

time spread, frequency diversity and temporal diversity are included to aid the UWB system. The performance of the system is dependent on the spreading gain factor.

Multipath and Inter-Symbol Interference

Multipath distortion is a type of interference occurring when a signal has more than one path between a transmitter and receiver. For example, a signal traveling may break up and reflect off different elements along a path. The reflected components of a signal can not only lose energy, but also arrive at the receiver at different times. Inter-Symbol Interference (ISI) and Inter-Block Interference (IBI) are related to multipath fading and synchronization errors. ISI is an effect where the energy from prior transmitted symbols in a bitstream is present in later symbols at the receiver. IBI is caused by the memory of a dispersive channel so that information from previous transmission blocks leak into the current one or information leaks from the succeeding block.

To eliminate ISI, one must insert a cyclic prefix and guard [9]. The prefix need only span more than the length of the channel impulse response to absorb the effects of ISI. Additionally, the guard sequence clears the channel memory after each block transmission. It should be emphasized that the output symbols containing interference (the prefix and guard symbols) are discarded at the receiver. Finally, at the receiver end, each truncated block is fast Fourier transform (FFT) processed so that the rest of the receiver software algorithms can be carried out. This is also shown in Figure 2.

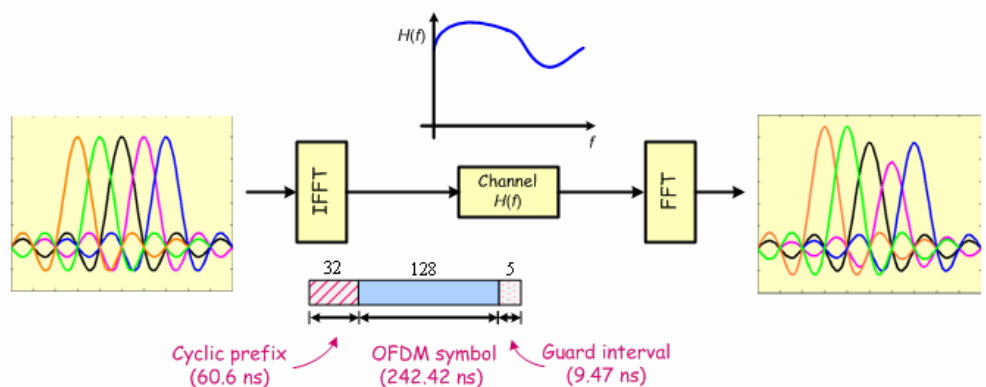


Figure 2: OFDM Modulation

UWB System

The UWB system data rates tested and the system's rate-dependent parameters can be seen in Table 1. It supports ten different data rates [2]. The low data rates, between 53.3 to 80 Mbps, have an overall spreading gain of 4 and a time spreading factor of 2. The middle data rates which exist from 106.7 to 200 Mbps possess an overall spreading gain of 2 with no frequency spread. There is no frequency spreading or time spreading in support of the high data rates which are above 200 Mbps.

Data Rate (Mb/s)	Modulation	Coding rate (R)	Conjugate Symmetric Input to IFFT	Time Spreading Factor	Overall Spreading Gain	Coded bits per OFDM symbol (N_{CBPS})
53.3	QPSK	1/3	Yes	2	4	100
55	QPSK	11/32	Yes	2	4	100
80	QPSK	1/2	Yes	2	4	100
106.7	QPSK	1/3	No	2	2	200
110	QPSK	11/32	No	2	2	200
160	QPSK	1/2	No	2	2	200
200	QPSK	5/8	No	2	2	200
320	QPSK	1/2	No	1 (No spreading)	1	200
400	QPSK	5/8	No	1 (No spreading)	1	200
480	QPSK	3/4	No	1 (No spreading)	1	200

Table 1: Rate-dependent parameters.

The UWB system consists of two parts: Baseband and Radio Frequency (RF). Figure 3A is a block diagram showing the baseband stages of the transmitter; the data scrambler, convolutional encoder and puncturer, bit-interleaver, constellation mapper, and inverse FFT. These stages are each handled in a C program. The baseband of the receiver (Figure 3B), generally, contains the reverse order of the transmitter stages.

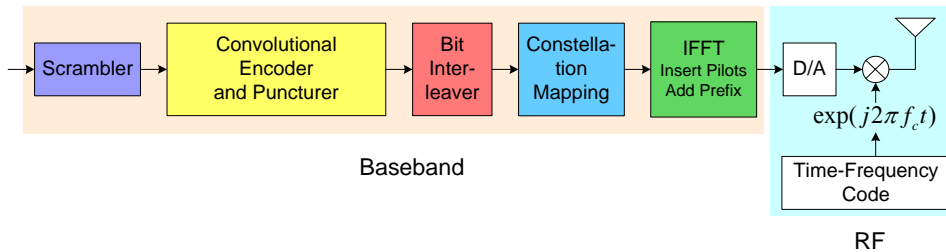


Figure 3A: Single-antenna multiband UWB-OFDM transmitter.

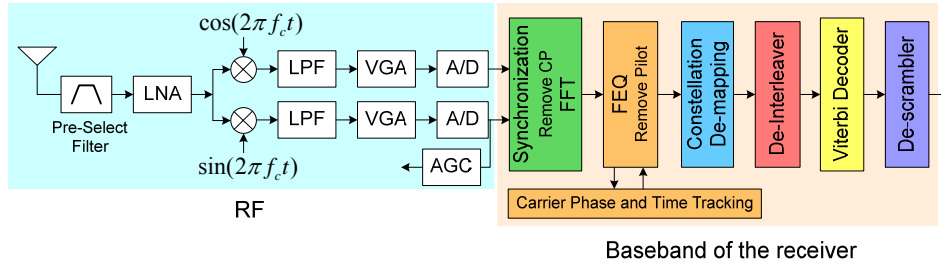


Figure 3B: Single-antenna multiband UWB-OFDM receiver.

In the first stage of the UWB system, the datastream is generated by using pseudo random binary sequence (PRBS) generator which, letting D be a single bit delay element, follows this equation:

$$g(D) = 1 + D^{14} + D^{15} \quad (3)$$

The scrambled data bits are obtained using:

$$s_n = b_n \oplus x_n \quad (4)$$

where

$$x_n = x_{n-14} \oplus x_{n-15} \quad (5)$$

and b_n is the unscrambled data bits. The \oplus denotes modulo-2 addition. The scrambler is designed to convert bit sequence into a pseudorandom sequence free from long strings of simple patterns like 1's or 0's in a transmitted signal. It is of great importance that the scrambler at the transmitter and de-scrambler at the receiver are initialized with the same seed value or else the stream at the receiver will be incorrect.

In the next stage, the convolutional encoder adds patterns of redundancy to the data in order to improve the signal-to-noise ratio (SNR) for more accurate decoding at the receiver. The coding rates of Table 1 refer to the number of bits transmitted. For example, our convolutional encoder's coding rates are $1/3$, $11/32$, $1/2$, $5/8$, and $3/4$ where $1/3$ is the mother coding rate. All the other coding rates are obtained by puncturing the mother code. A coding rate of $1/3$ means that for every 1 bit needing to be sent out, 3 bits are transmitted for redundancy. Puncturing is a procedure for omitting a block of encoded bits at the transmitter and inserting a 'dummy' zero bit in its place. The use of puncturing can significantly reduce the number of bits to be transmitted over the channel.

The Viterbi decoding algorithm [13] is utilized at the receiver to decode the convolutional encoded sequence.

The bit interleaving operation is performed in two stages: symbol interleaving and then tone interleaving. A bit interleaver is used to gain robustness against burst errors or losing consecutive data bits. Interleaving is performed on the coded bit stream so errors appear more randomly [9]. Figure 4 is a good illustration of the interleaving operation.

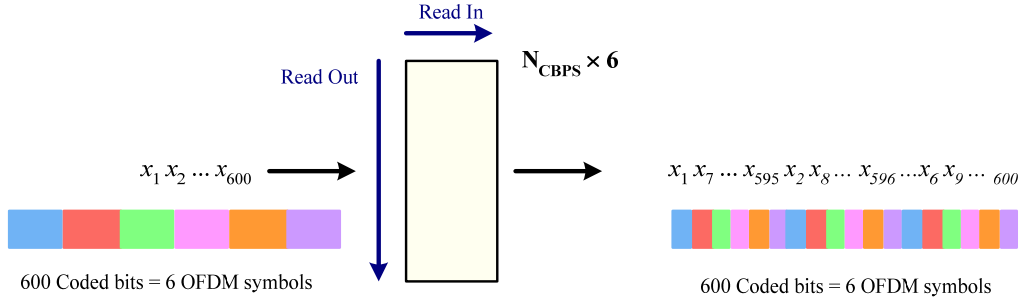


Figure 4A: Symbol Interleaving.

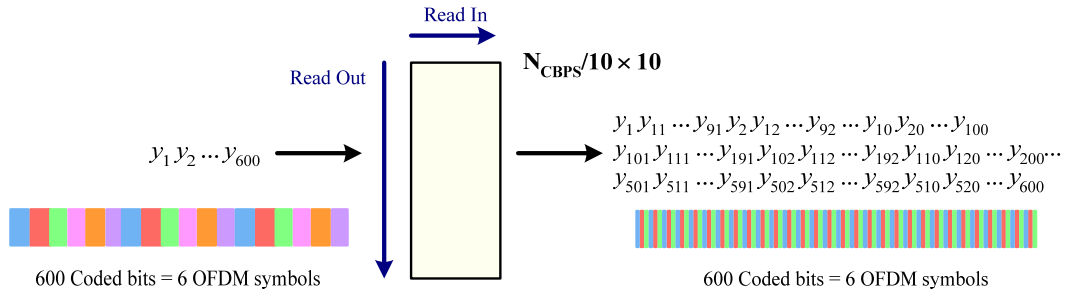


Figure 4B: Tone Interleaving.

Quadrature Phase Shift Keying (QPSK) is the phase modulation algorithm used in the constellation mapping step. In short, a cosine carrier is varied in phase while holding constant its amplitude and frequency. The input bit stream is converted into a complex stream using this equation:

$$d = (I + jQ) \times K_{MOD} \text{ where } K_{MOD} = 1/\sqrt{2} \quad (6)$$

and where I and Q are in-phase value I-out and quadrature value Q-out, respectively. The term "quadrature" in QPSK refers to the four phases, 45, 135, 225, and 315 degrees, in

which a carrier signal is sent (see Figure 5). Every two bits in a stream form one QPSK symbol.

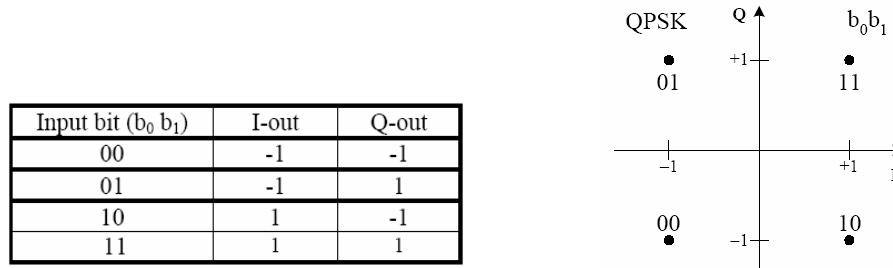


Figure 5: Constellation Mapping using QPSK modulation.

SISO, MISO, and MIMO UWB Systems

Three types of UWB multiband systems are covered in this paper. The system discussed in the above section represents the SISO system. The MISO and MIMO systems are obtained from modifying the SISO system. For the MISO system, the receiver will be the same, but the transmitter will have two antennas instead of one. For the MIMO system, the transmitter will be the same as that in MISO, but the receiver will now also have two antennas. In order to examine the performance each system, the bit-error-rate (BER) is observed with respect to the signal-to-noise ratio (SNR). In fact, the BER which depends on the coding gain and the diversity gain is actually proportional to SNR. SNR is calculated using the energy per symbol E_s and the noise energy N_0 :

$$SNR = \frac{1}{4}(E_s \cdot N_0) \quad (7)$$

Now, letting G_c be the coding gain and G_d be the diversity gain, the BER performance can be written as:

$$BER = (G_c \cdot SNR)^{-G_d} \quad (8)$$

The diversity and product criterion also play important roles in determining the performance of the system at high SNR and at low SNR.

Using the transmitted block code C_T and the received block code C_R , equation (9) shows how the number of antennas of the transmitter and receiver effect the performance of the system [11].

$$P(\mathbf{C}_T -> \mathbf{C}_R) \leq \left(\prod_{i=1}^n \lambda_i \right)^{-m} (SNR)^{-rm} \quad (9)$$

λ_i is the non-zero eigenvalues of $(\mathbf{C}_T - \mathbf{C}_R) \cdot (\mathbf{C}_T - \mathbf{C}_R)^H$ from λ_1 to λ_n where n is the number of transmitter antennas, m is the number of receiver antennas, and r is the rank.

Alamouti space-time block code (STBC) [1] is used in implementing the UWB MISO and MIMO systems since it has been proven as a 2-by-2 STBC which can achieve the full diversity for a system with two transmitters. An example of two transmitted symbols is demonstrated below:

LR, MR and HR are indications of low rate, middle rate and high rate.

$$\text{Transmitted_symbols} = \begin{pmatrix} x_1 \\ x_2 \end{pmatrix} \quad \text{Modulation_HR} = \begin{pmatrix} x_1 & x_2 \\ -x_2 & x_1 \end{pmatrix}$$

$$\text{Timespread_LR} = \begin{pmatrix} x_1 \\ x_2 \\ x_1 \\ x_2 \end{pmatrix} \quad \text{Modulation_LR \& MR} = \begin{pmatrix} x_1 & x_2 \\ -x_2 & x_1 \\ x_1 & x_2 \\ -x_2 & x_1 \end{pmatrix}$$

The difference between the SISO system and the MISO or MIMO system is the time spread scheme. In the SISO system, the duplicated symbol is transmitted in the next time slot. However, the MISO and MIMO systems use one antenna to transmit a symbol (x_1) and a conjugate symbol ($-x_2$) followed by the duplicated symbol and the duplicated conjugate. The additional antenna is used to transmit the other symbol (x_2) and the conjugate of x_1 . Alamouti is used to transmit the two symbols once the time spreading is applied. Based on the structure of Alamouti space-time block code, fast maximum likelihood (ML) detection [12], which is modified from Tarokh ML detection [10], is used at the receiver to demodulate the transmit signal.

UWB Standard Channel Models and Channel Estimation

There are four distinctive UWB standard channel models, designated as CM1, CM2, CM3, and CM4, which are specified in the IEEE 802.15.3a [5]. Each model is based on transmission distance and line-of-sight (LOS) conditioning, a term used by RF

technologies to describe an unobstructed path between the location of the signal transmitter and the location of the signal receiver. According to the definition of LOS in the Webopedia's website, obstacles which can cause an obstruction in the line of sight include trees, buildings, mountains, hills and other natural or manmade structures or objects. CM1 possesses the line-of-sight (LOS) multipath channel condition and is based on a distance of 0 to 4 meters between the transmitter and receiver. CM2 involves the same distance as CM1, but applies a non LOS (NLOS) condition instead. CM3 also operates on the NLOS condition, but on a transmission distance of 4 to 10 meters. Finally, CM4 implies a 4 to 10 meter transmission with an extreme NLOS condition.

A channel estimator is needed to assess time-varying amplitudes and phases of subcarrier channels. The channel can be calculated by using this equation :

$$H(f) = \frac{R(f)}{X(f)} \quad (10)$$

where $R(f)$ is the received signal in the frequency domain and $X(f)$ is the preamble and pilot sequence. Pilot symbols are inserted in the time and frequency dimensions to help form the channel estimate. The quality of channel estimation often depends on the number of pilots and their positions within the OFDM symbol [9]. However, while increasing the number of pilots may improve the estimate, it will also result in a loss of spectral efficiency. 6 zeroes are used as the pilot symbols for our UWB systems.

Adding the cyclic prefix described earlier drives the linear convolution to resemble a circular convolution [4]. Since a circular convolution in time is equivalent to a simple multiplication operation in frequency (equations 1 and 2), one channel tap is enough to nullify the effects of a multipath channel.

Matlab Implementation

Although the software was written in the C programming language and the hardware for the UWB system is in development by Maryland Semiconduct Inc. (MSI), the software, which included all the algorithms of the transmitter and receiver, was also written for Matlab for the purpose of running realistic simulations. Modifications were made to the existing Matlab software written by Hung-Quoc Lai in order to reflect the distortions discussed earlier.

The experiments for all three systems were carried out in the following way. A random bit sequence of n bits (chosen by the user) is generated and inputted to the UWB transmitter software algorithms. The output of the transmitter is passed through the standard channel models in another function. This is inputted into the receiver software. Finally, the BER was calculated by comparing the original random bitstream with the reconstructed bit sequence outputted by the receiver. Although this may sound simple, results took hours and eventually even days to be obtained.

Previously, to test all the software algorithms, Quoc had only multiplication of the transmitted information and the channel in the frequency domain to simulate the signal passing through a channel. To facilitate ISI testing, the transmission to the receiver program needed to be carried out in the time domain. In Quoc's experiment, there was no distinction between the resulting BERs for the four channels. Therefore, the group added Inverse Digital Fourier Transforms (IDFT) at the output of the transmitter and Digital Fourier Transforms (DFT) at the input of the receiver via the IFFT and FFT functions. Additionally, the multiplication in frequency was replaced by a time convolution after and before the IFFT and FFT matlab functions respectively.

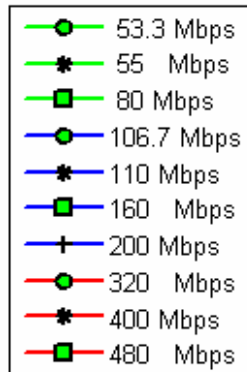
The presense of the time convolution meant the addition of ISI distortion. Therefore, a cyclic prefix matrix of 32 by N , the number of OFDM symbols, was inserted before 'transmission' and discarded after the time convolutions for the receiver. It will be interesting to see if OFDM is as robust against ISI as it is claimed to be.

Channel estimation was also inserted since the real system would need to perform the calculation. Initially, the channels in frequency were found by simply Fourier transforming the channels made in the time domain. A function was written by the group to take a known time sequence called a preamble and convolve it twice with a time channel. The average of the two convolutions was taken to account for noise interference. Of course, a prefix and guard needed used in the 'transmission' as well. After the convolution, the Fourier transform of the convolution was divided by the known preamble (in the frequency domain) to obtain the transfer function of the frequency channel. This was used in the random bitstream simulations to find the transmitted signal from the received signal at the receiver. Additionally, the position of the pilots was altered in experiments in order to find the best resulting figures.

First, simulations were run with ideal conditions such as no noise and ideal channels, 1's for the frequency channel and a delta dirac function for the time channel. Once the preliminary testing was finished and bugs were removed, simulations were run so that each data rate was tested for all three systems over four distinct channels in order to calculate a BER for 11 SNRs (dB). By completing 5 consecutive transmissions with a random bitstream of 50,000 bits, an average BER for each SNR, data rate, and channel was found. The resulting numbers were used to make smooth plots of the behavior of the BER with respect to transmission parameters.

Results

The plots for the SISO, MISO, and MIMO systems under the four standard channel models with ISI and noise, but no channel estimation are shown in Figures 6 to 8. For each plot, the y-axis is a logarithmic scale of the BER running from 10^{-3} to 1 and the x-axis is a linear scale of the SNR in dB starting at 0 and ending with 20. Each data rate is designated in the legend below. Green indicates low data rates, blue connotes the middle data rates, and the high data rates are represented by the color red.



Legend: The data rates for the plots in the Results section

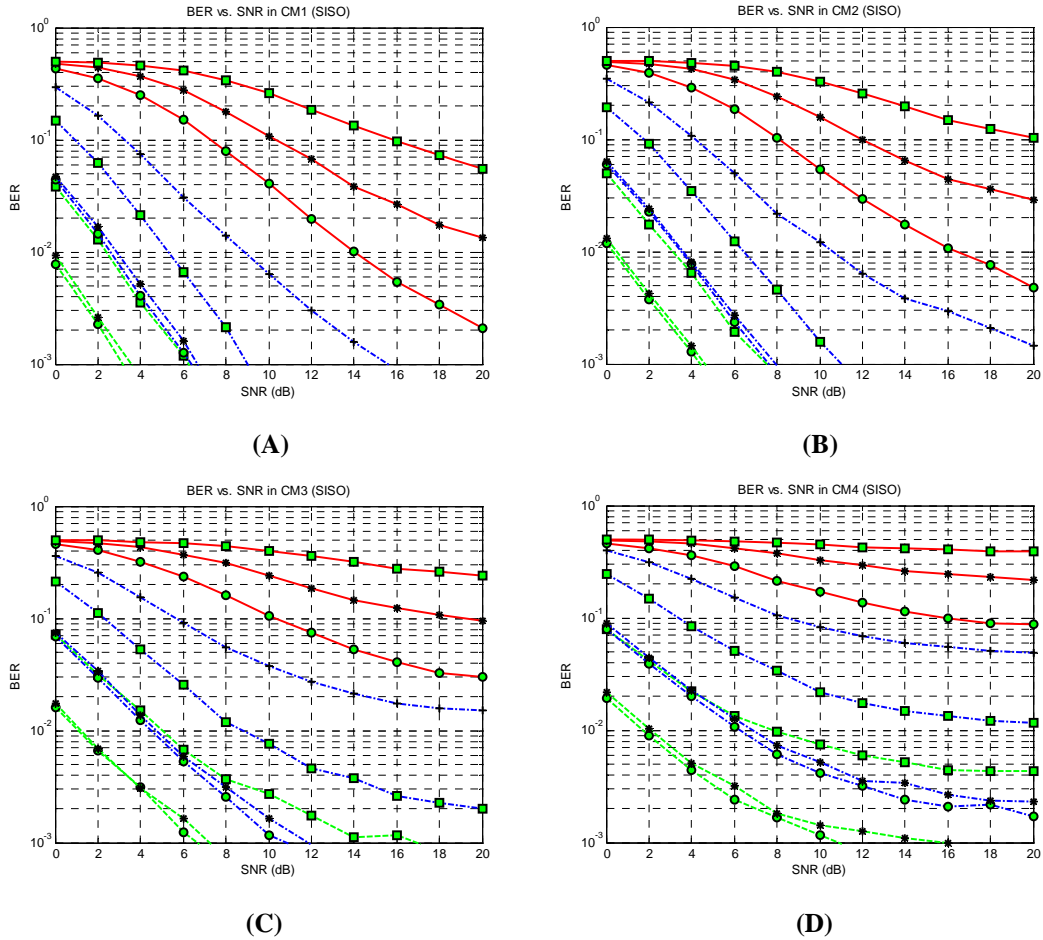
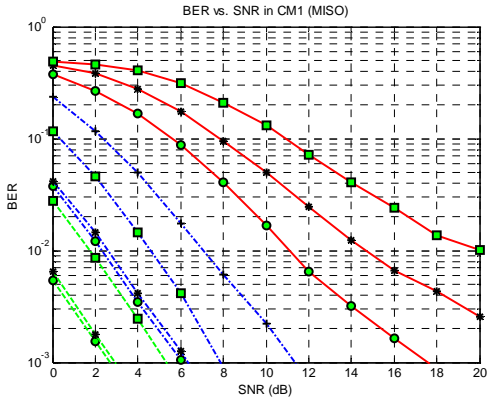
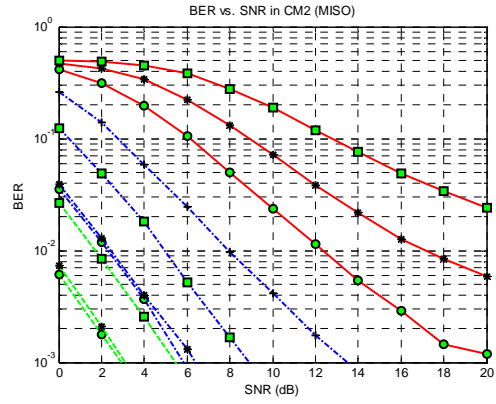


Figure 6: SISO BER vs. SNR plots for (A) CM1, (B) CM2, (C) CM3, and (D) CM4 without channel estimation.

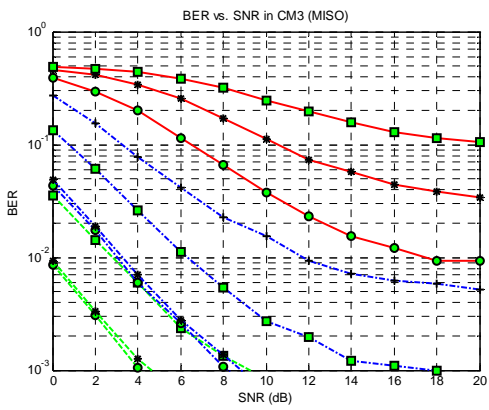
Figure 6 shows that the SISO system performs best over channel 1 and the worst over channel 4. The lower data rates have BERs that eventually reach zero. However, the middle data rates for channel 4 and the high ones for all the channels never have a BER of zero. In fact, even at an SNR of 20, the BER for 480 Mbps over CM4 is approximately 39 %. The negative slopes of the data rates clearly increase in each consecutive channel as well.



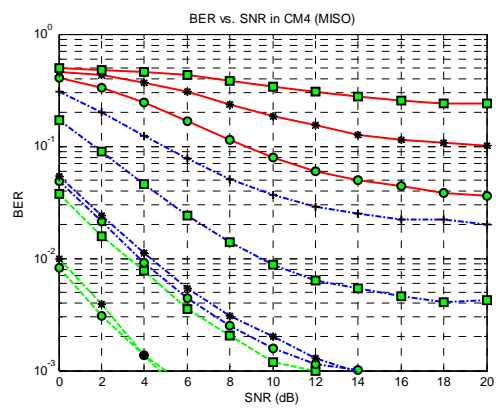
(A)



(B)

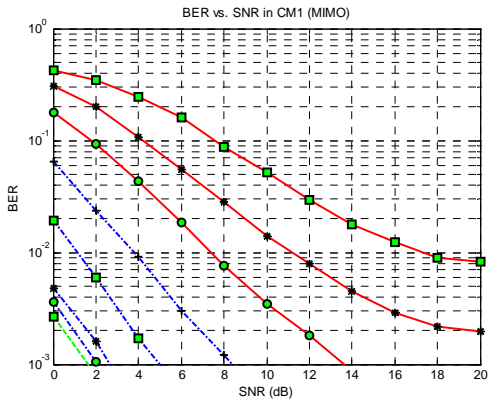


(C)

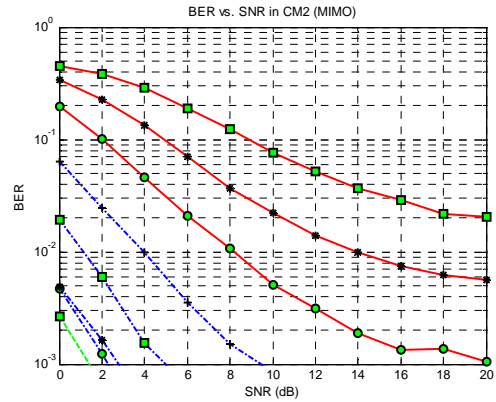


(D)

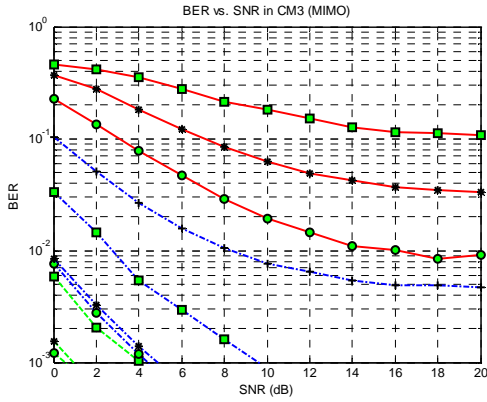
Figure 7: MISO BER vs. SNR plots for (A) CM1, (B) CM2, (C) CM3, and (D) CM4 without channel estimation.



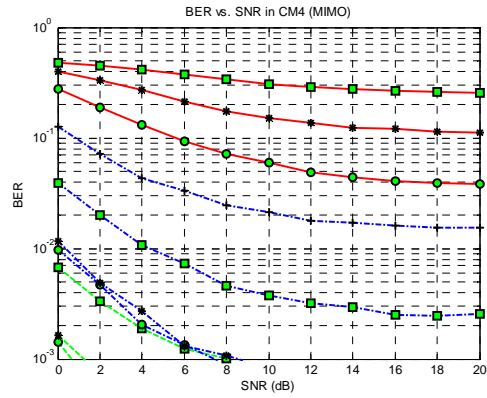
(A)



(B)



(C)

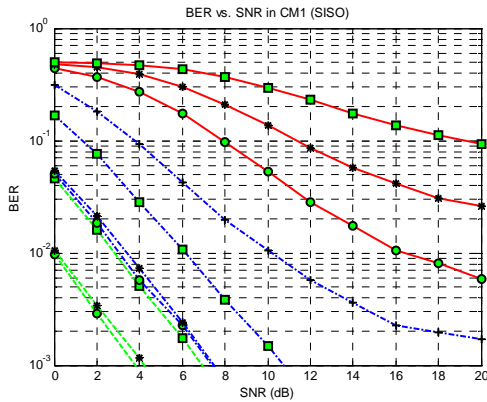


(D)

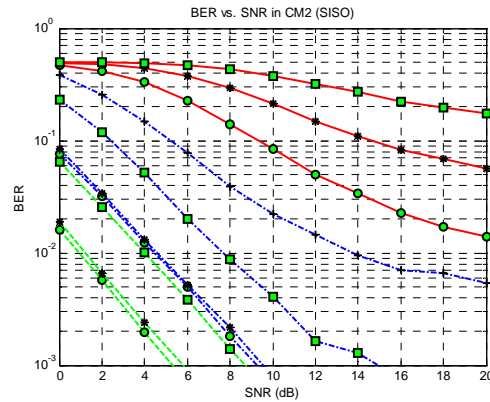
Figure 8: MIMO BER vs. SNR plots for (A) CM1, (B) CM2, (C) CM3, and (D) CM4 without channel estimation.

In the SISO system, as the data rate increases, at the same SNR, the bit error rate also increases. The type of behavior shown in the SISO system exists for the other two systems as well except the BERs show greater improvement. The MISO and MIMO plots are shown in Figures 9 and 10 respectively. In these systems, the lower data rates reach zero BER much more quickly and more of the middle data rates reach zero. Both systems even boast zero BERs for a high data rate (320 Mbps) in CM1 and CM2.

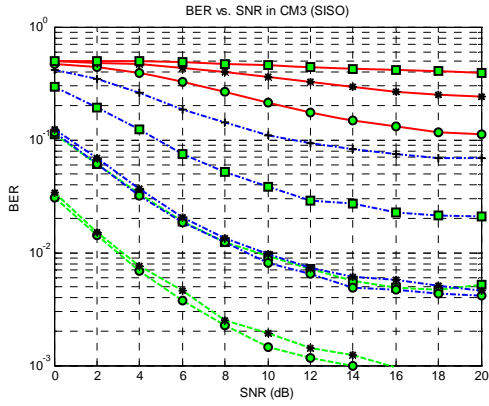
In addition to ISI and noise, Figures 9, 10, and 11 are the BER vs. SNR plots for all the data rates of the SISO, MISO, and MIMO system with channel estimation.



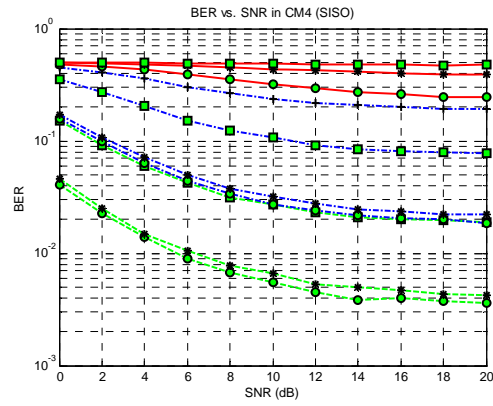
(A)



(B)

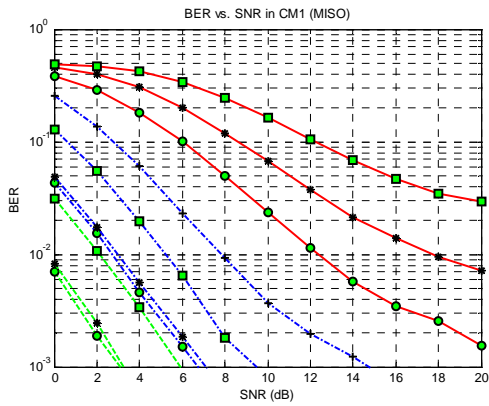


(C)

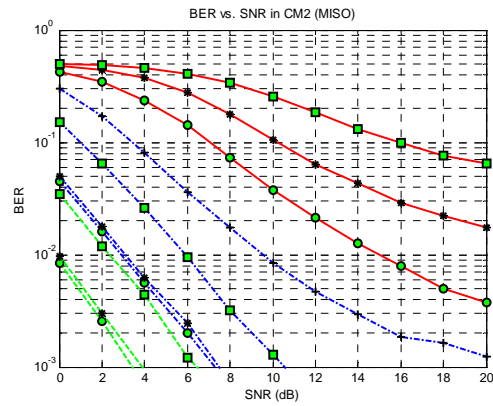


(D)

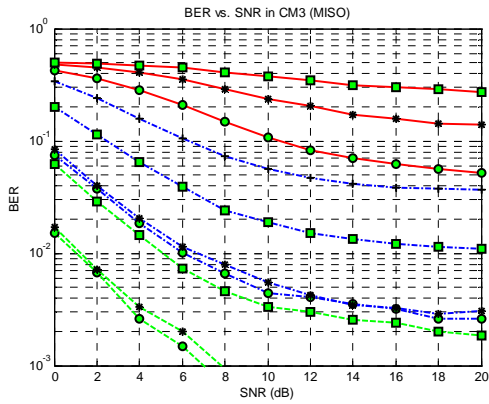
Figure 9: SISO BER vs. SNR plots for (A) CM1, (B) CM2, (C) CM3, and (D) CM4 with best channel estimation.



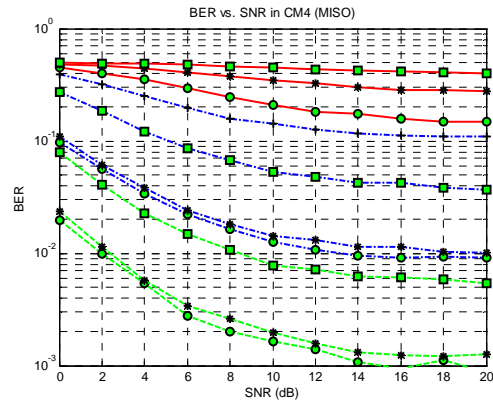
(A)



(B)



(C)



(D)

Figure 10: MISO BER vs. SNR plots for (A) CM1, (B) CM2, (C) CM3, and (D) CM4 with best channel estimation.

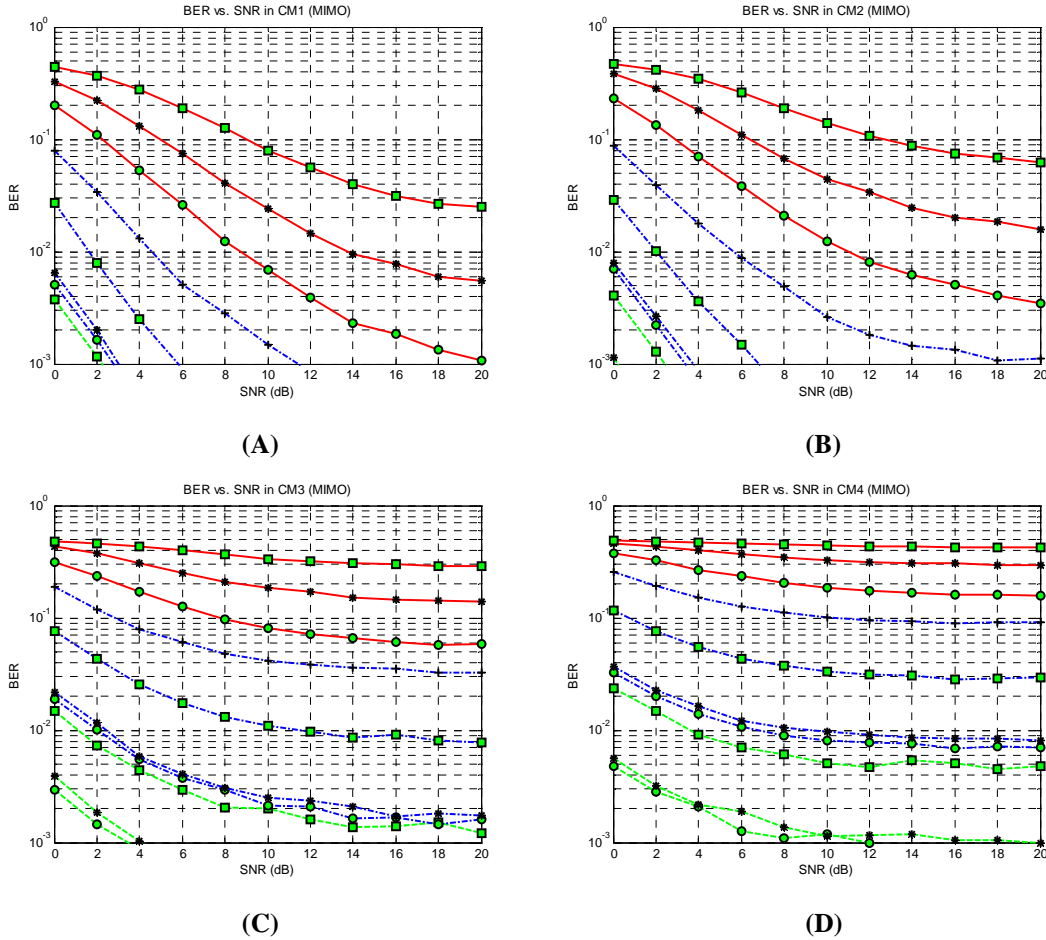


Figure 11: MIMO BER vs. SNR plots for (A) CM1, (B) CM2, (C) CM3, and (D) CM4 with best channel estimation.

When comparing Figures 6 through 8 with Figures 9 to 11, the addition of channel estimation undeniably affects all 3 systems. While the deterioration isn't seen as much in CM1, the other channels worsen more and more. For instance, the BER never reaches zero even for the lowest data rates in channels 3 and 4. However, like before, the behavior of the BER continues to show improvement when comparing each consecutive system.

Discussion

The actions of each system can be explained and were certainly anticipated. At low SNR, each system obviously performs worse than high SNR since the noise power is closer to the signal power. Thus, the signal gets altered more over the channel, making it more difficult to discern the original at the receiver. The lower data rates operate better than the middle and higher data rates for a reason as well. As was written before, the low

data rates (53.3 – 80 Mbps) held frequency and temporal diversity gain so it's as if the receiver has more information to determine each transmitted symbol. The middle data rates (106.7 – 200 Mbps) held only a temporal diversity gain and, hence, the receiver got nearly twice the information present at the high data rate transmission. With two or four times the information, the receiver can reconstruct the original bit sequence with much greater ease. This is especially the case at high SNRs because the additional information will more closely resemble the previous info with less noise distortion.

As expected, the MIMO system outperformed MISO and SISO. The difference can really be seen in channels 1 and 2 for MIMO where, essentially, the low data rates have a BER of zero at almost all SNRs. The middle rates of MIMO actually behave more like the lower rates of SISO. Figure 9A and 11A show that, at a data rate of 160 Mbps and 10^{-2} BER, the MIMO system achieves a performance improvement of about 4.5 dB. It's really only in the highest data rates passing over channel 3 and 4 where MIMO doesn't trounce the original system. Figures 9D and 11D show that MIMO's improvement over SISO is about 8 dB for 320 Mbps at a 0.3 BER. However, even in that case, one must keep in mind the small slope of the data rates over the 20 dB SNR range. MIMO's victory can be easily explained by its antenna scheme which gives the system the highest spatial diversity gain of four. MISO has a spatial diversity of two and SISO only has a spatial diversity of one, which is considered no gain at all. Mathematically, it is the diversity criterion which is responsible for the slope of the asymptotic performance.

The inclusion of the channel estimation affected the performance of all three systems. However, it should also be noted that the channel estimation employed was very basic. Due to time constraints, channel estimation did not use the algorithms at the transmitter and receiver to ensure the best signal recovery. It is certainly possible to obtain a better estimate.

Although they were not included in the Results section, other results existed for channel estimation as well. When the position of the pilot symbols (zeroes) was altered in the program, the BER performance was quite different. Our initial tests with 3 pilots at the beginning of the preamble and 3 at the end yielded satisfying results (see the Appendix for these figures). However, they were neither the best nor the worst. In fact, there was even a strange occurrence with this case that goes against one would expect.

For all three systems, the 80 Mbps data rate was outperformed by 106.7 and 110 Mbps in CM3 and CM4. This can be explained. Referring to equation (8), one sees that the coding gain and diversity gain are important factors for the BER. In CM3 and CM4, the effect of ISI can be so great that the coding gain would dominate that of diversity gain. This would damage performance the BER at 80 Mbps.

Better results had to be found. The best channel estimation figures (shown in the Results section) were found by adding one pilot to the beginning of the preamble and 5 to the end. The odd data rate behavior was fixed. It seemed as though the worst results for channel estimation came when zeroes were added into the middle of the preamble.

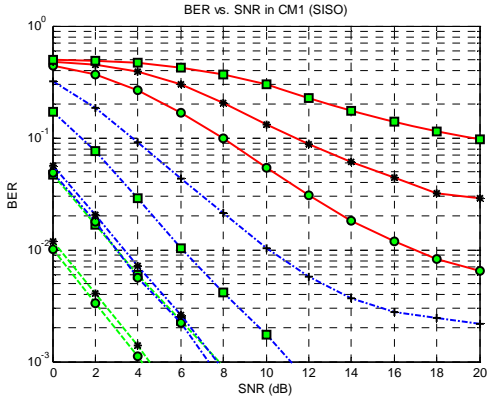
Inter-Symbol Interference had great effects on the BER for all the data rates, especially the highest. Before ISI was added to the program, all the channels gave the same curve for all three systems. Clearly, this did not make any sense in the real world since Line-of-Sight (LOS) and transmission distance should affect system performance.

Although the high data rates, particularly 480 Mbps and 400 Mbps, did not have impressive results for CM3 and CM4, they did hold up better in the MIMO system across CM1 and CM2. Therefore, it is safe to say that UWB systems can achieve success at the highest data rates depending on the application and channel estimation used. However, for the time being, users may only be able to utilize high data rates over short ranges with less obstacles.

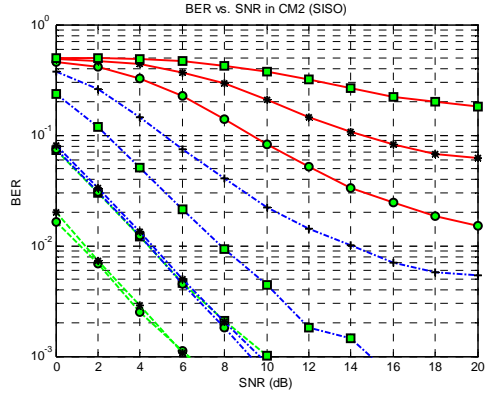
Conclusion

Results show that Orthogonal Frequency Division Multiplexing is a very capable form of modulation for Ultra-WideBand systems. Its high spectral efficiency and prevention against many distortions is proven. Additional antennas at the transmitter and receiver only boosted the performance of UWB systems. Also, while ISI and channel estimation can affect UWB transmission, they do not deteriorate UWB performance enough to reduce its importance for home and office applications. Generally, MIMO outperformed SISO by approximately 4 dB for all the data rates in CM1, but the improvement was greater in CM4 ranging from about 8 to 12 dB. Since a real UWB system will probably operate in the SNR range of 2 to 6 dB, results show that the BER of each system at high data rates is between 30% and 50% which is inadequate for the majority of applications over long ranges. It also was very fascinating to discover that a lower data rate did not necessarily show better results than middle data rates in certain cases. In the future, better forms of channel estimation should be applied in simulations and other types of distortion need to be tested to see whether UWB technology still maintains acceptable performance.

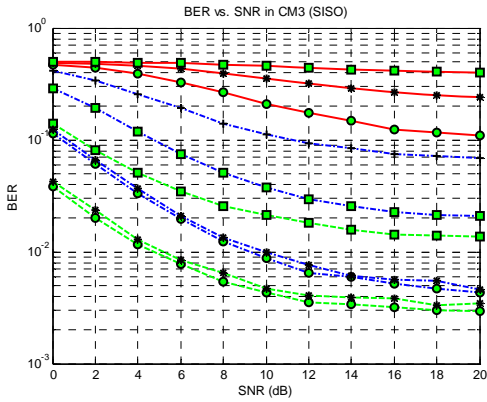
Appendix



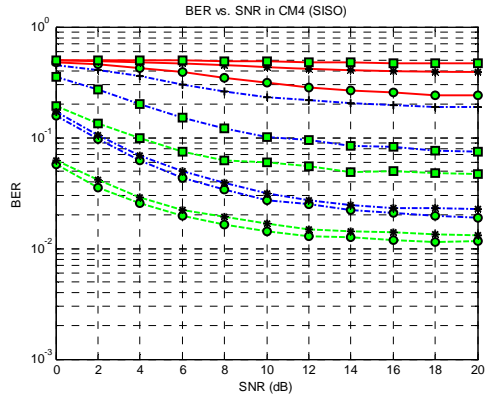
(A)



(B)

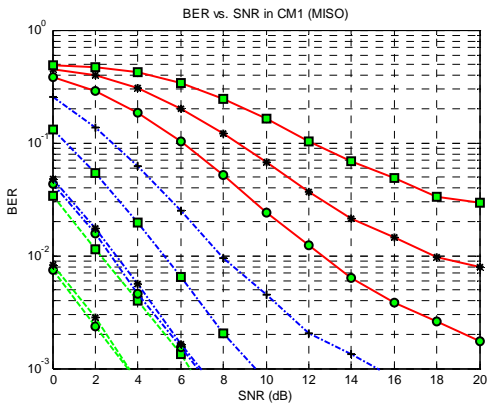


(C)

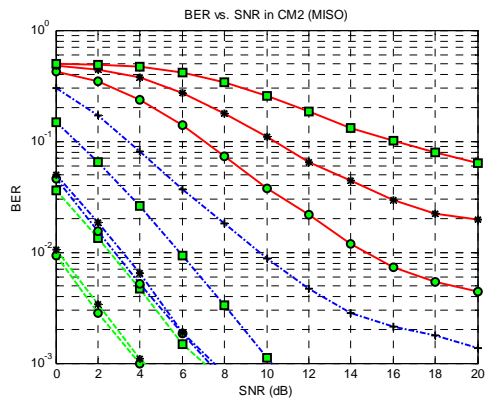


(D)

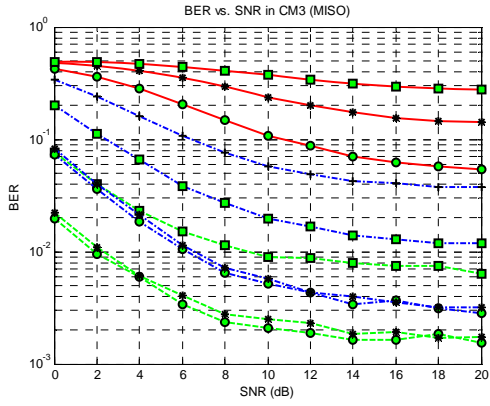
SISO BER vs. SNR plots for (A) CM1, (B) CM2, (C) CM3, and (D) CM4 with original channel estimation.



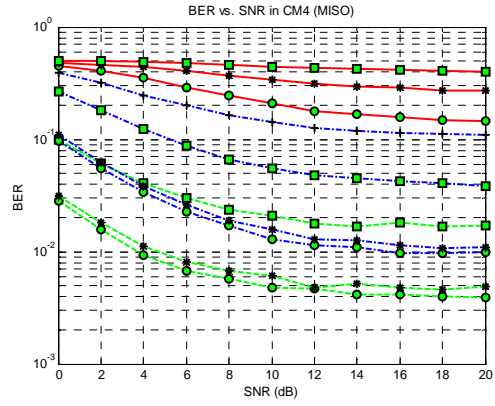
(A)



(B)

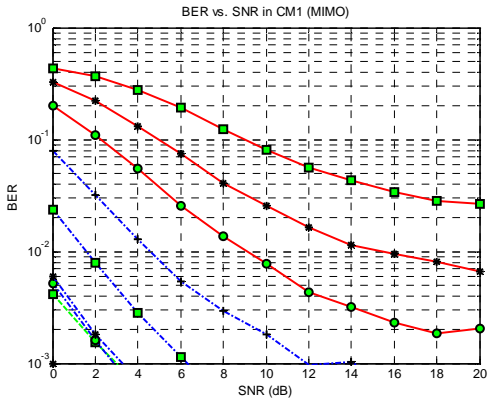


(C)

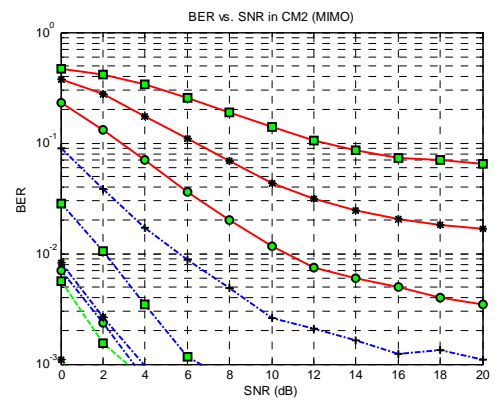


(D)

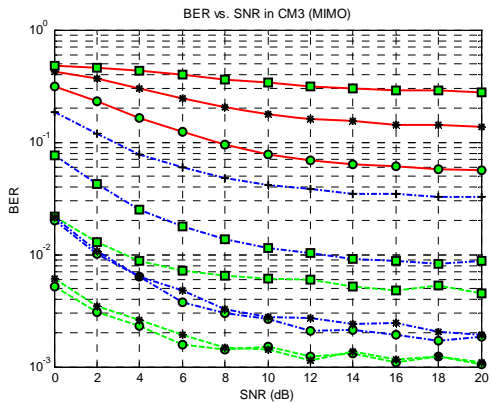
MISO BER vs. SNR plots for (A) CM1, (B) CM2, (C) CM3, and (D) CM4 with original channel estimation.



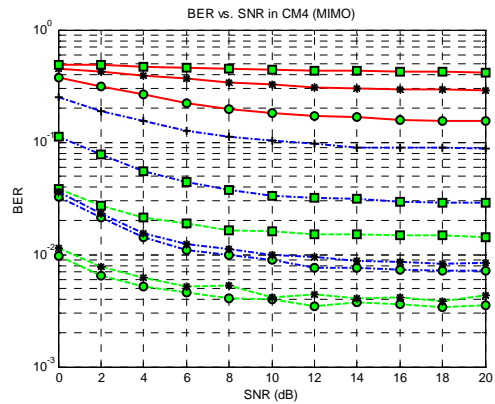
(A)



(B)



(C)



(D)

MIMO BER vs. SNR plots for (A) CM1, (B) CM2, (C) CM3, and (D) CM4 with original channel estimation.

References

- [1] S.M. Alamouti, "A simple transmitter diversity scheme for wireless communications," *IEEE J. Select. Areas Commun.*, vol. 16, pp. 1451-1458, Oct. 1998.
- [2] A. Batra, et. al., "Multi-band OFDM Physical Layer Proposal for IEEE 802.15 Task Group 3a," *IEEE P802.15-03/268r3*, Mar. 2004.
- [3] Communications Commission Report FCC 02-48, Revision of Part 15 of the Commission's Rules Regarding Ultra Wideband Transmission Systems, First Report and Order;
http://www.fcc.gov/Bureaus/Engineering_Technology/Orders/2002/fcc02048.pdf
- [4] M. Debbah, "Short Introduction to OFDM," Internet presentation;
www.eurecom.fr/~debbah/papier/ofdm/tutorial.pdf
- [5] J. Foerster, et. al., "Channel Modeling Sub-committee Report Final," *IEEE P802.15-02/368r5-SG3a*, July 2004
- [6] K. J. Ray Liu's group, "Design high-speed wireless USB using the emerging ultra-wideband transmission techniques," MIPS project, Department of Electrical and Computer Engineering and Institute for System Research University of Maryland at College Park, 2005.
- [7] G. M. Maggio, "Introduction to UWB", Internet presentation;
http://inls.ucsd.edu/~lev/ws2003/WS2003_UWB.pdf
- [8] A. F. Molisch, et. al., "Channel models for ultrawideband personal area networks," *IEEE Wireless Commun.*, pp. 14-21, Dec. 2003.
- [9] K. Pietikainen, "Orthogonal Frequency Division Multiplexing", Internet presentation;
http://www.comlab.hut.fi/opetus/333/2004_2005_slides/ofdm_text.pdf
- [10] R. Roberts, "XtremeSpectrum CFP Document," *IEEE P802.15-03/154r1*, Mar. 2003.
- [11] V. Tarokh, et. al., "Space-time codes for high data rate wireless communication: Performance criterion and code construction," *IEEE Trans. Inform. Theory*, vol. 44, pp. 744-765, Mar. 1998.
- [12] V. Tarokh, et. al., "Space-time block coding for wireless communications: Performance results," *IEEE J. Select. Areas Commun.*, vol. 17, no.3, pp. 451-460, Mar. 1999.

- [13] A. Viterbi, "Error Bounds for Convolutional Coders and Asymptotically Optimum Decoding Algorithm," IEEE Trans. On Information Theory, vol. 13, pp. 55-67, Apr. 1967.